ESI:

Multidentate Polar Interactions Enable Ultralow-Dosage Electrolyte Additives for Stabilizing Zn-I_2 Batteries

Junlin Shi[†, a], Jiapei Li[†, b], Yongze Kan [a], Shuilin Wu [a, *]

[a] Key Laboratory of Catalysis and Energy Materials Chemistry of Ministry of Education & Hubei Key Laboratory of Catalysis and Materials Science, South-Central Minzu University, Wuhan 430074, China

E-mail: wushuilin@mail.scuec.edu.cn

[b] Department of Materials Science and Engineering, and Center of Super-Diamond and Advanced Films, City University of Hong Kong, 83 Tat Chee Avenue, Hong Kong, China

[†] These authors were equally contributed.

I. Methods

Electrolyte Preparation: The chemicals are commercially purchased from Macklin® and used as revived, which are zinc sulfate heptahydrate ($ZnSO_4 \cdot 7H_2O$, 99.5% purity, CAS: 7446-20-0), D-Glucosamine sulfate ($C_6H_{15}NO_9S$, 98% purity, CAS:29031-19-4). In terms of the concentration, the 1 m denotes 1 molar salts dissolved in per kilogram water.

Preparation of the iodine cathode: The iodine cathodes were prepared by mixing iodine (I_2, purchased from HEOWNS®) and activated carbon (purchased from XF Nano®) with a mass ratio of 6:4, followed by thermal treatment in a sealed vessel at 100°C for 8 h. After cooling, the resulting composite was mixed with additional activated carbon and polytetrafluoroethylene (60 wt% aqueous dispersion, Aladdin®) at a mass ratio of 80:15:5 to form a homogeneous slurry. The slurry was then rolled into a thin film (~200 μm thickness) with an areal I_2 mass loading of ~20 mg cm^{-2}, punched into 12 mm circular discs and pressed into Ti mesh for testing.

Test methods: The Coulombic efficiency (CE) of repetitive Zn stripping/plating was evaluated using Zn-Cu asymmetric cells. Specifically, the cells were first discharged at a designated current density (e.g., 1 mA cm^{-2}) for a fixed duration, followed by charging at the same current density to a cutoff voltage of 0.5 V on Newware® battery testing system. The CE was calculated as the ratio of charge time to discharge time. The galvanic corrosion rate of Zn was evaluated based on Zn-Cu galvanic cells. The differential capacitance of the Zn foil in Zn-Zn symmetric cells was determined by cyclic voltammetry (CV) within a potential window of -10 to 10 mV at various scan rates. And the differential capacitance at each scan rate was calculated from the anodic-cathodic current difference according to: $C_{diff} = (i_a - i_c)/2v$, where i_a and i_c are the anodic and cathodic current densities at the same potential, and v is the scan rate. Linear sweep voltammetry (LSV) was performed in a three-electrode system with titanium as the working electrode, and Zn as both the counter electrode and the reference electrode. Tafel plots were measured via Zn-Zn symmetric cells. These tests were conducted using a Correst® multi-channel electrochemical workstation. Electrochemical impedance spectroscopy (EIS) measurements were performed on a Donghua® electrochemical workstation over a frequency range of 100 kHz to 100 mHz with an AC amplitude of 10 mV. The electrochemical performance of Zn-I_2 cells was evaluated by cyclic

voltammetry and galvanostatic charge-discharge techniques within a voltage range of 0.5 V-1.6 V.

Characterization: Fourier transform infrared (FTIR) spectra were acquired on a Nicolet iS50 spectrometer over the wavenumber range of 4000-400 cm^{-1} with a resolution of 4 cm^{-1} at ambient temperature, and the attenuated total reflection (ATR) mode was employed for sample testing. Field-emission scanning electron microscopy (FE-SEM) was utilized to observe the microscopic morphology and structural features of the samples, which was performed on a Zeiss Sigma 300 instrument at an accelerating voltage of 5-15 kV. All samples were mounted on conductive adhesive substrates and underwent gold sputtering treatment before characterization to improve electrical conductivity. X-ray photoelectron spectroscopy (XPS) measurements were conducted on a Thermo ESCALAB 250Xi spectrometer with monochromatic Al Kα X-ray radiation to investigate the surface elemental composition and chemical valence states. All binding energies were calibrated relative to the C 1s peak at 284.8 eV, and high-resolution XPS spectra were fitted to differentiate various chemical bonding environments.The Ultraviolet-visible (UV-vis) spectra were collected using a UV1900 instrument (Shimadzu, Japan).

Theoretical simulations: All density functional theory (DFT) calculations were performed using CP2K program package with the Quickstep module, which employs the Gaussian and plane wave (GPW) method. The CP2K input file was generated using Multiwfn 3.8. The system was treated under periodic boundary conditions in the *x* and *y* directions, with a vacuum layer of 15-20 Å added along the *z*-axis to avoid interactions between periodic images. The electronic structure was described using the generalized gradient approximation (GGA) with the Perdew-Burke-Ernzerhof (PBE) exchange-correlation functional. Grimme's DFT-D3 (BJ) dispersion correction was applied to account for van der Waals interactions. Core electrons were represented using norm-conserving Goedecker-Teter-Hutter (GTH) pseudopotentials, and valence electrons were expanded in DZVP-MOLOPT-SR-GTH basis sets. A plane-wave cutoff of 400 Ry and a relative cutoff of 55 Ry were used. The DIIS (direct inversion in the iterative subspace) minimizer and full preconditioner were used to ensure efficient SCF convergence. Smearing was applied using the Fermi-Dirac method with an electronic temperature of 300 K to facilitate electronic convergence for the metallic system. The convergence threshold for the SCF cycles was set to 1.0×10^{-6}. Geometry optimization

was performed using the Broyden-Fletcher-Goldfarb-Shanno (BFGS) algorithm with convergence thresholds of 4.5×10^{-4} Ha/Bohr for maximum force, 3.0×10^{-4} Ha/Bohr for RMS force, 3.0×10^{-3} Bohr for maximum displacement, and 1.5×10^{-3} Bohr for RMS displacement. The adsorption energy was calculated using the following equation:

$$E_{ads} = E_{surface+absorbate} - E_{surface} - E_{adsorbate}$$

Where $E_{surface+absorbate}$ is the total energy of the optimized surface with the adsorbate particle. $E_{surface}$ is the total energy of the clean, relaxed surface. $E_{adsorbate}$ is the energy of the isolated adsorbate particles calculated in a sufficiently large vacuum box.

II. Figures and Tables:

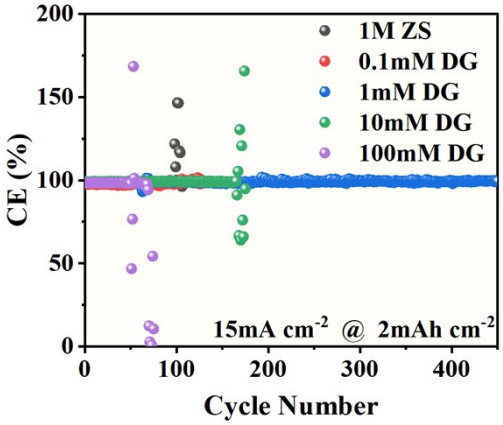

Fig. S1 Electrochemical performance of Zn metal anodes in 1 M $ZnSO_4$ electrolyte with DG additive: Coulombic efficiency of Zn-Cu cells at 15 mA cm^{-2} with an areal capacity of 2 mAh cm^{-2}.

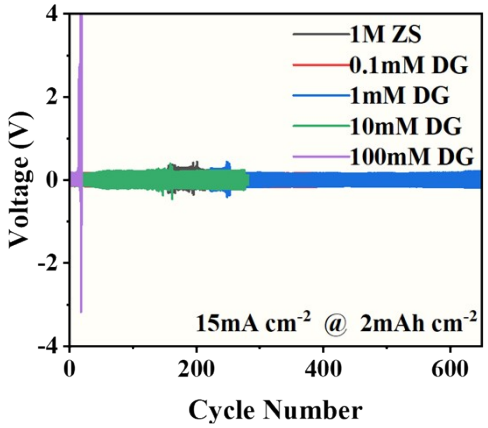

Fig. S2 Electrochemical performance of Zn metal anodes in 1 M $ZnSO_4$ electrolyte with DG additive: voltage profiles of Zn-Zn symmetric cells cycled at 15 mA cm^{-2} with an areal capacity of 2 mAh cm^{-2}.

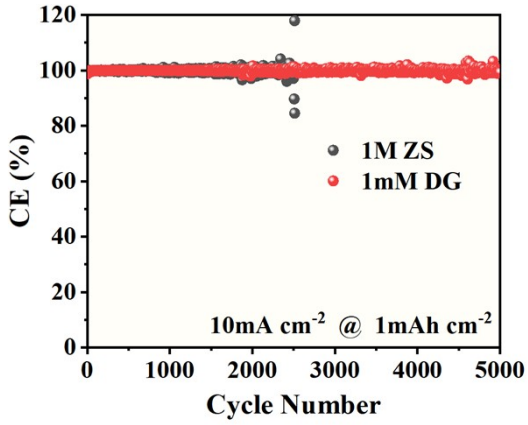

Fig. S3 Coulombic efficiency of Zn-Cu cells at 10 mA cm^{-2} with an areal capacity of 1 mAh cm^{-1}.

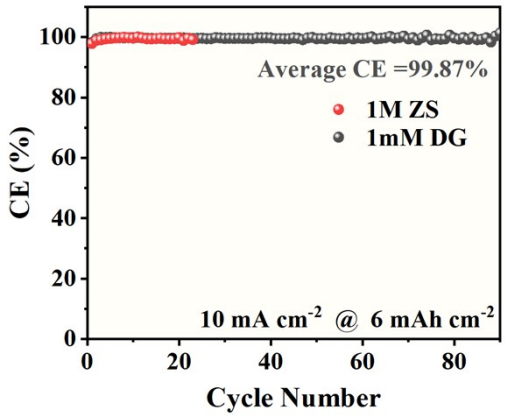

Fig. S4 Coulombic efficiency of Zn-Cu cells at 10 mA cm^{-2} with an areal capacity of 6 mAh cm^{-1}.

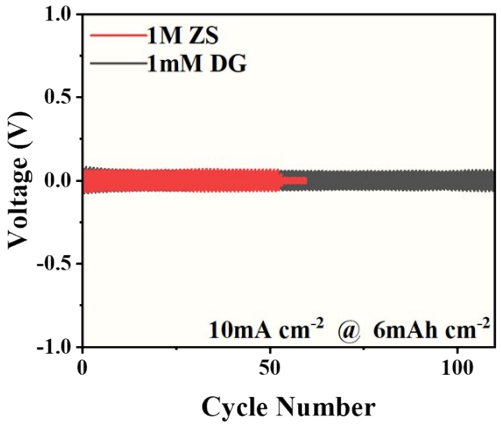

Fig. S5. Voltage profiles of Zn-Zn symmetric cells cycled at 10 mA cm^{-2} with an areal capacity of 6 mAh cm^{-2}.

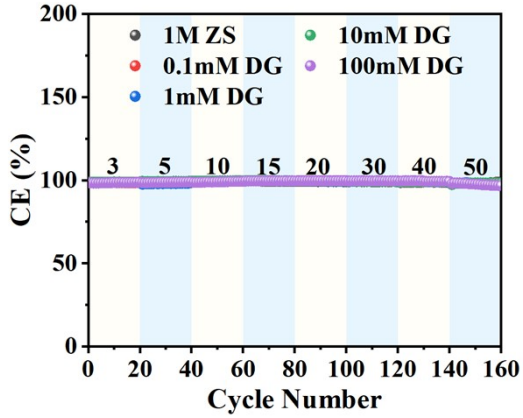

Fig. S6 Rate performance in Zn-Cu cells (1 M $ZnSO_4$ with 0.1-100 mM DG).

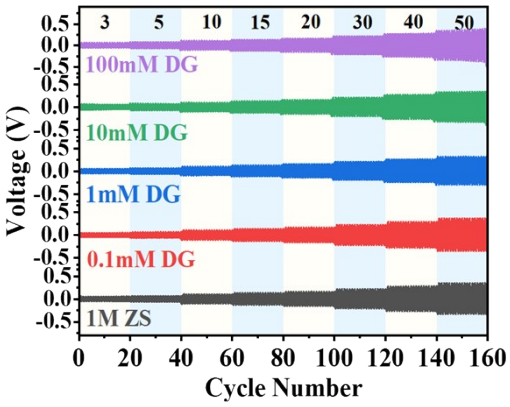

Fig. S7 Rate performance in Zn-Zn symmetric cells (1 M $ZnSO_4$ with 0.1-100 mM DG).

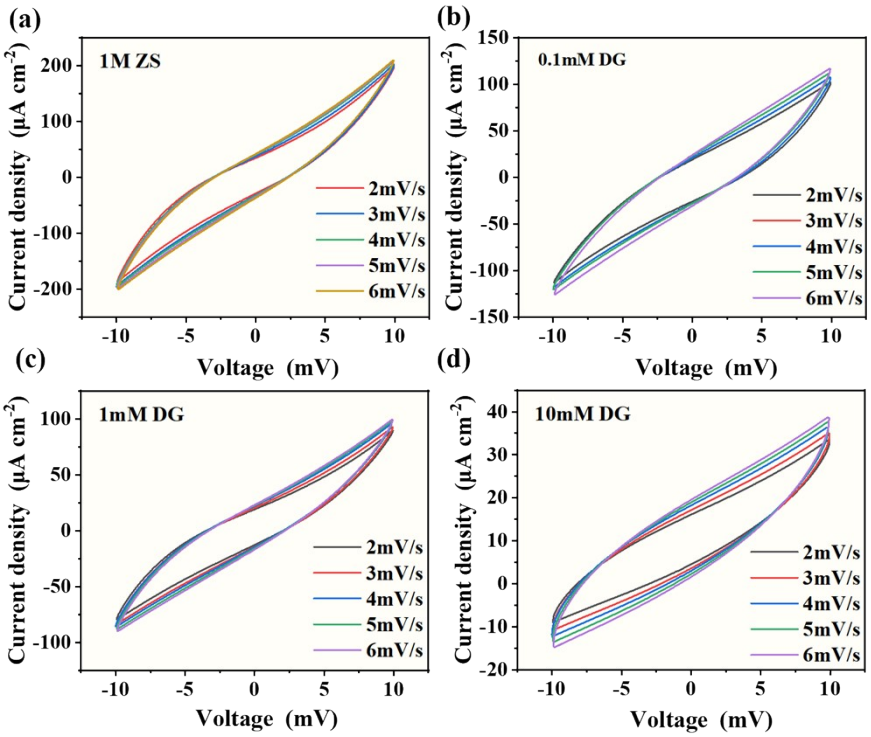

Fig. S8 Measurement of electrochemical double-layer capacitance in electrolytes with different concentrations of D-glucosamine sulfate. Cyclic voltammetry (CV) curves of Zn-Zn batteries at various scan rates (2-6 mV s^{-1}) within the voltage range of -10 to 10 mV:(a) 1M ZS(b) 0.1mM DG (c) 1mM DG (d) 10mM DG.

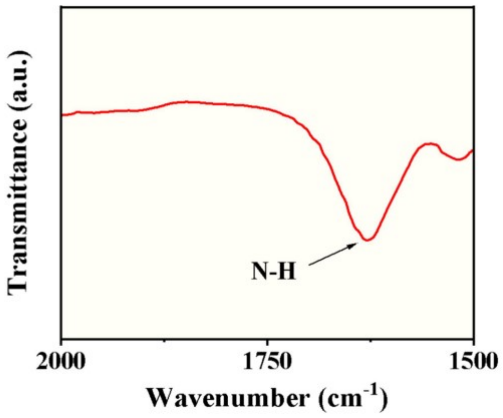

Fig. S9 The Fourier transform infrared spectra (FT-IR) of Zn anode after cycling.

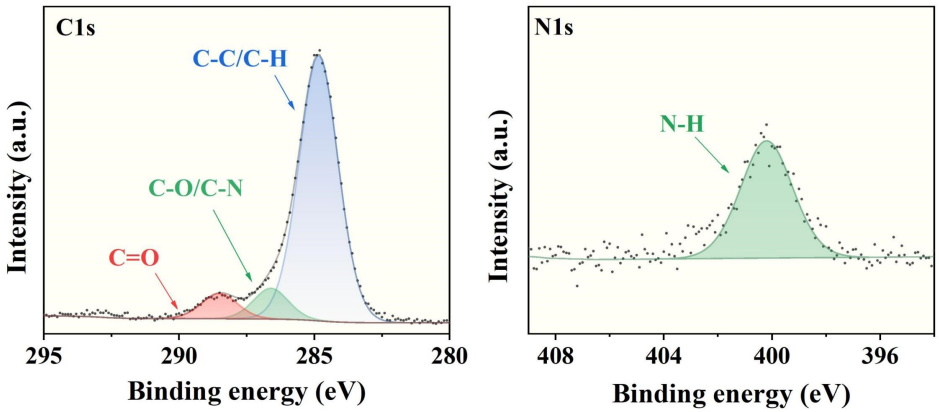

Fig. S10 The XPS depth profiles for C 1s and N1s of Zn anode surface after cyclin.

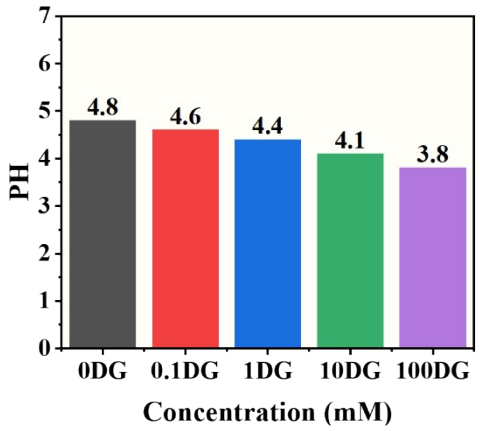

Fig. S11 PH values of electrolytes with different concentrations of D-glucosamine sulfate.

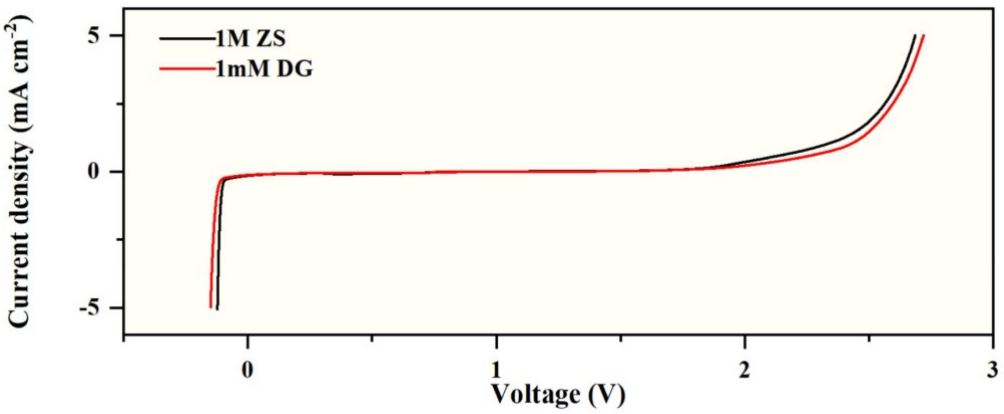

Fig. S12 Linear Sweep Voltammetry of 1 M ZS and 1mM DG.

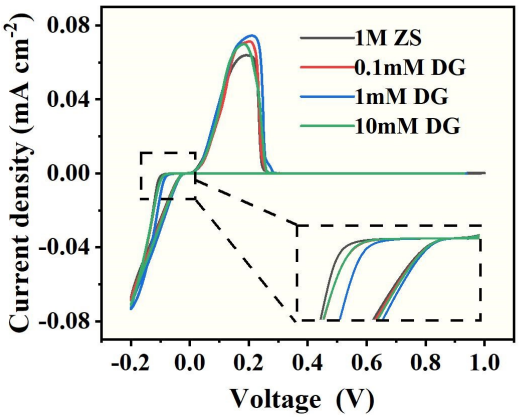

Fig. S13 Cyclic voltammetric (CV) curves of Zn-Cu cells in electrolytes with different concentrations of DG.

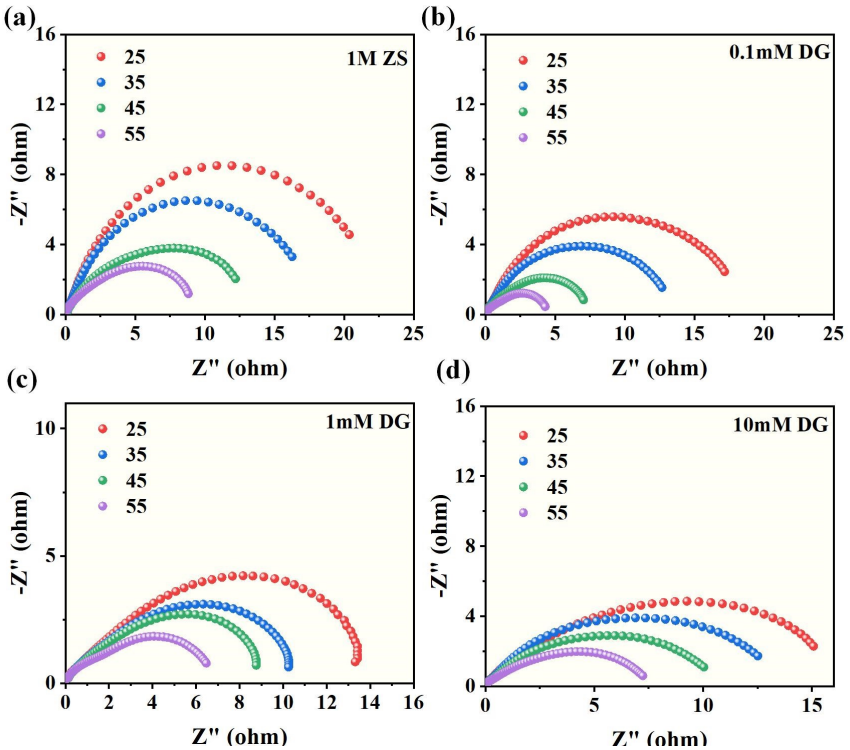

Fig. S14 Electrochemical impedance spectra (EIS) of Zn-Zn symmetric cells as a function of temperature:(a) EIS of 1 M ZS (b) EIS of 0.1mM DG (c) EIS of 1mM DG (d) EIS of 10mM DG.

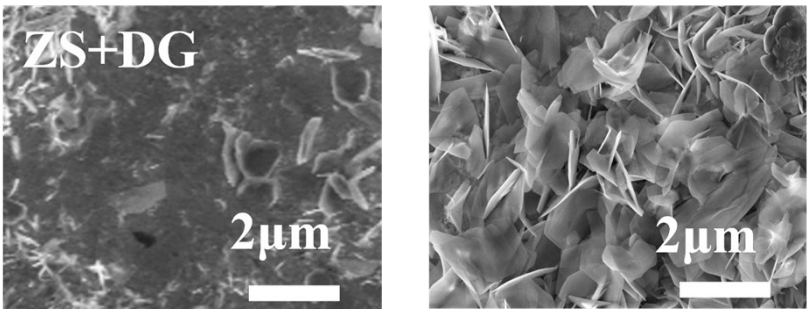

Fig. S15 SEM images of Zn deposition in ZS and ZS+DG electrolytes.

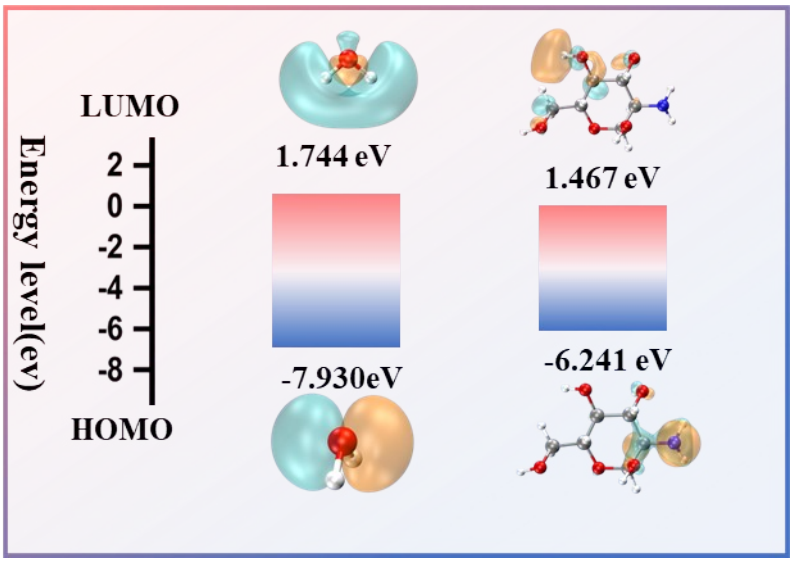

Fig. S16 HOMO-LUMO energy levels of DG and water, schemetics of mechanisms.

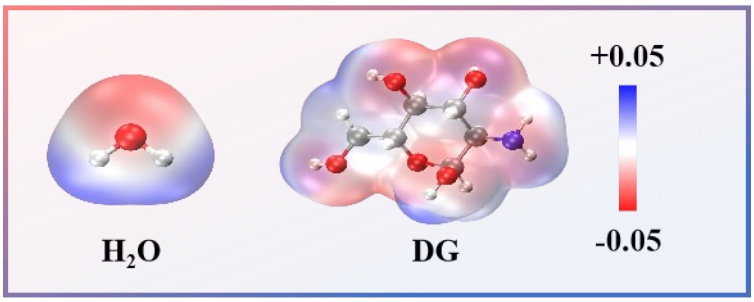

Fig. S17 Electrostatic potential mapping of the DG and H_2O.

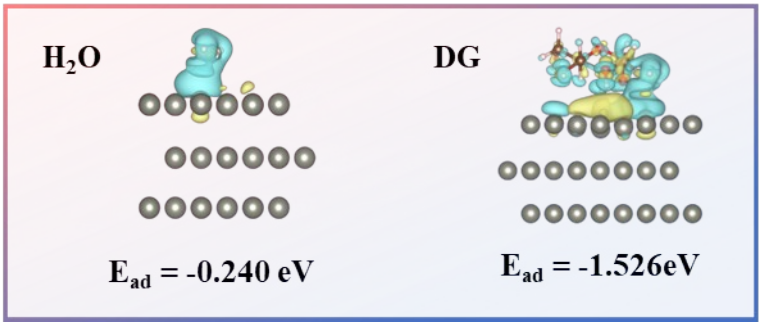

Fig. S18 The 3D charge density difference of DG and H_2O on the Zn (002) plane.

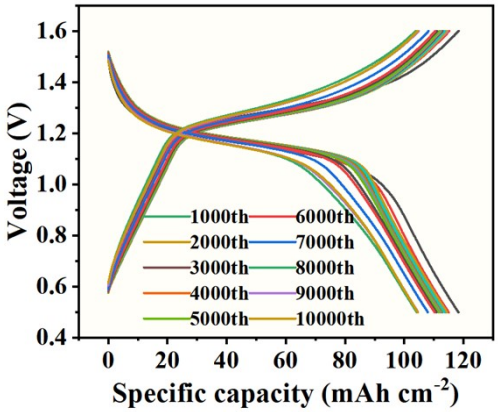

Fig. S19 Corresponding charge-discharge curves at specific cycles.

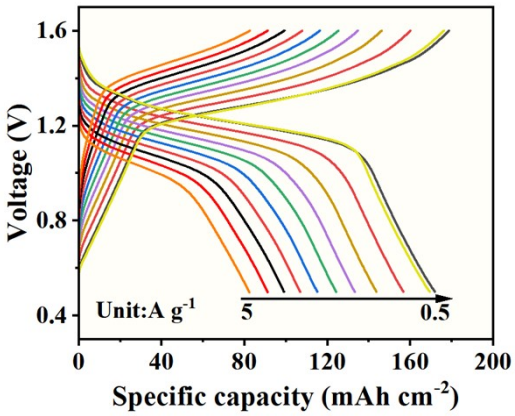

Fig. S20 Corresponding charge-discharge profiles.

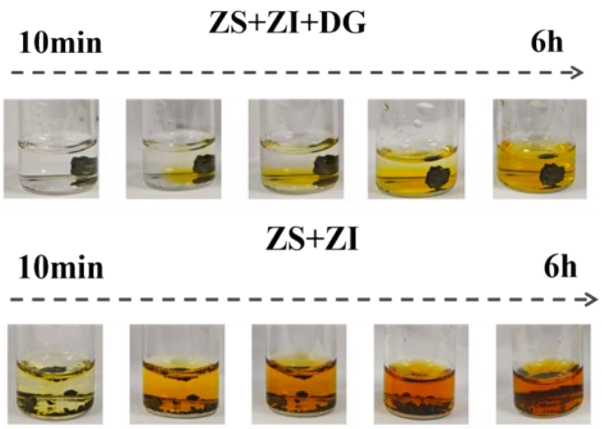

Fig. S21 Temporal evolution of color of the ZS+ZI solution and ZS+ZI+DG solution after iodine addition.

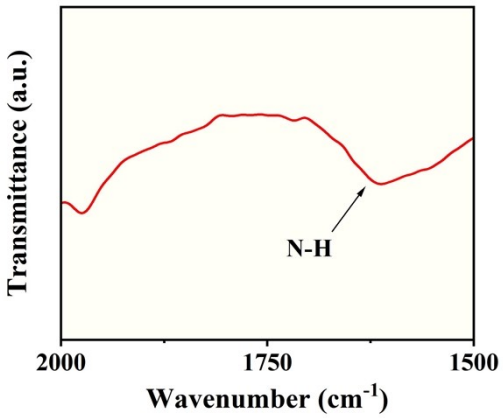

Fig. S22 The Fourier transform infrared spectra (FT-IR) of I_2@AC anode after cycling.

Table S1. . Performance comparison in Zn-ion batteries with high specific capacity and additive prices

Electrolyte system	Additive price	Cycling stability	Reference
KMO// $ZnSO_4$+SF-H_2O//Zn	1231820 ¥/L	170 mAh g^{-1} @ 3 A g^{-1} / % (1000 cycles)	ACS Nano.2022
PANI// $ZnSO_4$+SG-H_2O//Zn	26257.78 ¥/L	99.5 mAh g^{-1} @ 5 A g^{-1} 81.7% (1400 cycles)	Adv. Mater.2022
MnO_2// $ZnSO_4$+TC-H_2O//Zn	1624.48 ¥/kg	150 mAh g^{-1} @ 0.5 A g^{-1} 67% (680 cycles)	Adv. Energy. Mater.2022
MnO_2// $ZnSO_4$+CTAB-H_2O//Zn	2406.55 ¥/kg	126.56 mAh g^{-1} @ 4 A g^{-1} / % (1000 cycles)	Adv. Funct. Mater. 2023
V_2O_5//$ZnSO_4$+AQS-H_2O//Zn	2092 ¥/kg	/ @ 5 A g^{-1} 92% (500 cycles)	Angew. Chem. Int. Ed. 2023
I_2//$ZnSO_4$+BHEG-H_2O//Zn	1798 ¥/kg	158.7 mAh g^{-1} @ 2 A g^{-1} 87.9% (8000 cycles)	Adv. Mater.2024
ZVO// $ZnSO_4$+N-ac-H_2O//Zn	4516.8 ¥/kg	/ @ 5 A g^{-1} 78.75% (2000 cycles)	J. Am. Chem. Soc. 2024
MnO_2// $ZnSO_4$+SnI_4-H_2O//Zn	22690 ¥/kg	290 mAh g^{-1} @ 1 A g^{-1} 98% (800 cycles)	Chem. Eng. J.2025
VO_2//$ZnSO_4$+ZP-H_2O//Zn	5000 ¥/kg	/ @ 1 A g^{-1} 73.8% (1000 cycles)	*A*dv. Funct. Mater. 2025
MnO_2// $ZnSO_4$+EMC+MA-H_2O//Zn	9390 ¥/kg 881 ¥/L	/ @ 1 A g^{-1} 89.9% (700 cycles)	J. Am. Chem. Soc. 2025
AVO// ZnOTF+LACT-H_2O//Zn	29640 ¥/kg	133 mAh g^{-1} @ 10 A g^{-1} 91.66% (2000 cycles)	J. Colloid Interface Sci. 2026
I_2//$ZnSO_4$+DG-H_2O//Zn	**1560 ¥/kg**	**110 mAh g^{-1} @ 2 A g^{-1} 92% (10000 cycles)**	***This work***